

Defect-concentration dependence of electrical transport mechanisms in CuO nanowires

Zufang Lin^a, Runze Zhan^a, Luying Li^b, Huihui Liu^c, Shuangfeng Jia^c, Huanjun Chen^a,
Shuai Tang^a, Juncong She^a, Shaozhi Deng^a, Ningsheng Xu^a and Jun Chen^{a*}

- State Key Laboratory of Optoelectronic Materials and Technologies, Provincial Key Laboratory of Display Material and Technology, School of Electronics and Information Technology, Sun Yat-sen University, Guangzhou, 510275 China
- Wuhan National Laboratory for Optoelectronics, Huazhong University of Science and Technology, Wuhan, 430074 China
- School of Physics and Technology, Center for Electron Microscopy, Wuhan University, Wuhan, 430072 China

*E-mail: stscjun@mail.sysu.edu.cn

S1. Resistance of the Ni electrode. We experimentally measured the resistance of the Ni electrode, and the result is presented in Fig. S1; it shows that the resistance of the Ni electrode was approximately 100 Ω , which has no impact on the electrical-property measurements results of the CuO nanowires.

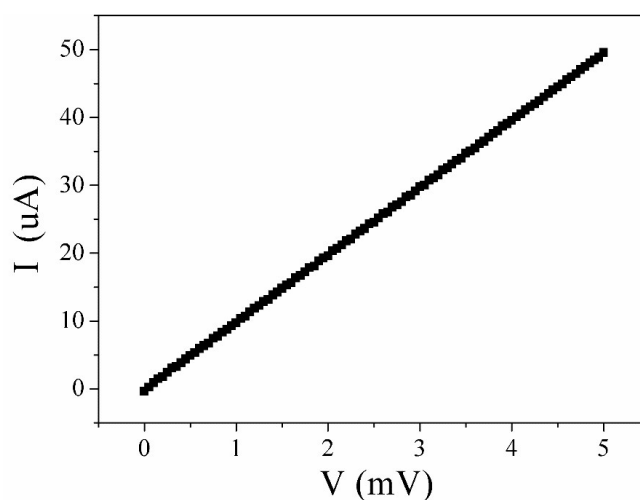


Fig. S1 *I-V* curve of the Ni electrode.

S2. X-ray photoelectron spectroscopy (XPS) result for a 10-nm-thick surface-etched Ni electrode. The result shown in Fig. S2 demonstrates that it is Ni, rather

than NiO, that makes contact with the nanowires.

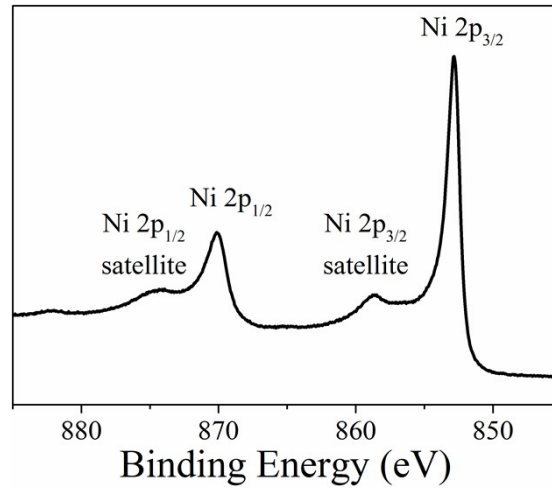


Fig. S2 XPS result for the surface-etched Ni electrode.

S3. Statistical conductivities of nanowires with different electrode materials. Fig. S3 shows the statistical results for the conductivities of samples measured using Au (black squares) or Ni (red dots) as the electrodes. Both kinds of samples have the same range of conductivities.

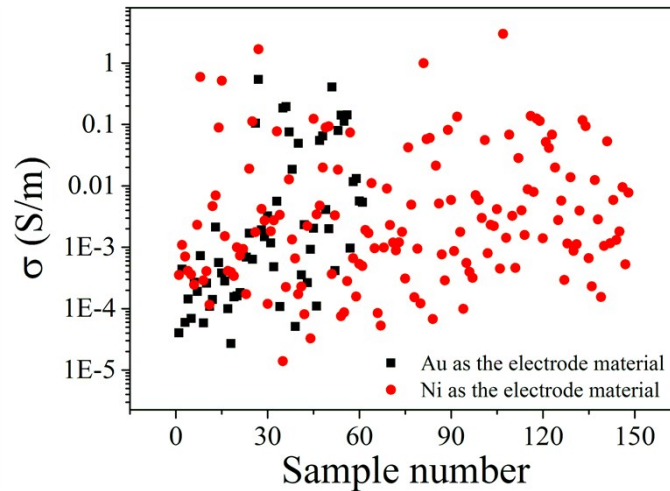


Fig. S3 Statistical results for the conductivities of samples measured using Au (black squares) or Ni (red dots) as the electrodes.

S4. Typical fitting results using the back-to-back Schottky conduction mechanism. In the back-to-back Schottky conduction mechanism, the current density can be described by the following equation:¹

$$J(V) = \frac{J_1 J_2 \sinh(qV/2k_B T)}{J_1 \exp(qV/2n_1 k_B T) + J_2 \exp(-qV/2n_2 k_B T)}, \quad (1)$$

where $J_{1,2} = A * T^2 \exp(q\phi_{B_1, B_2} / k_B T)$, ϕ_{B_1, B_2} are the barrier heights of the contacts, V is the applied voltage, and $n_{1,2}$ is the ideality factor. The fitting result for one of the samples is shown in Fig. S4. By changing the values of ϕ_{B_1, B_2} and $n_{1,2}$, we obtained the best-fit result using $\phi_{B_1} = 0.60$ eV, $\phi_{B_2} = 0.95$ eV, $n_1 = 1.01455$, and $n_2 = 1.39842 \times 10^6$. From the fitted result, however, it is clear that the back-to-back Schottky model does not fit our data. Moreover, the work functions of Ni ($\Phi=4.99$ eV) and CuO ($\Phi=4.78$ eV²) indicate that Ohmic contact can be obtained, and the step of thermal annealing also helps to remove mid-gap states at the interface, both of which benefit the formation of Ohmic contact. Therefore, the back-to-back Schottky mechanism can be excluded.

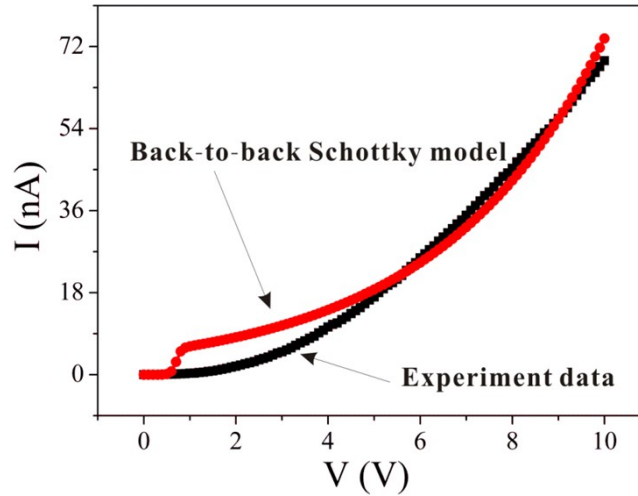


Fig. S4 Typical fitting result for one of the samples using the back-to-back Schottky conduction mechanism.

S5. Relationship between the conductivity and the diameter and contact lengths of the samples. The results plotted in Fig. S5 show that the conductivity is not influenced by the diameter or contacted length of the nanowires.

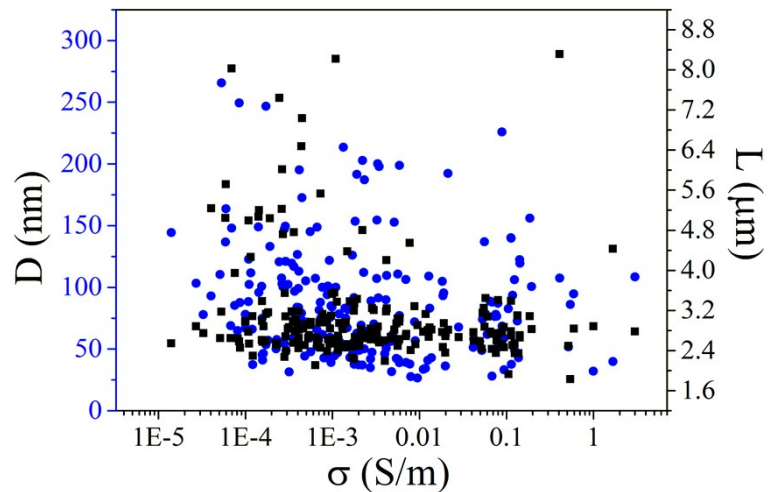


Fig. S5 Relationship between the conductivity and the diameter and contact length of the nanowires.

S6. Simulation results of the SAED pattern of type III sample. The SAED pattern shows the good crystal quality of the nanowire, with extra diffraction spots attributed to diffraction from the nanoparticles.

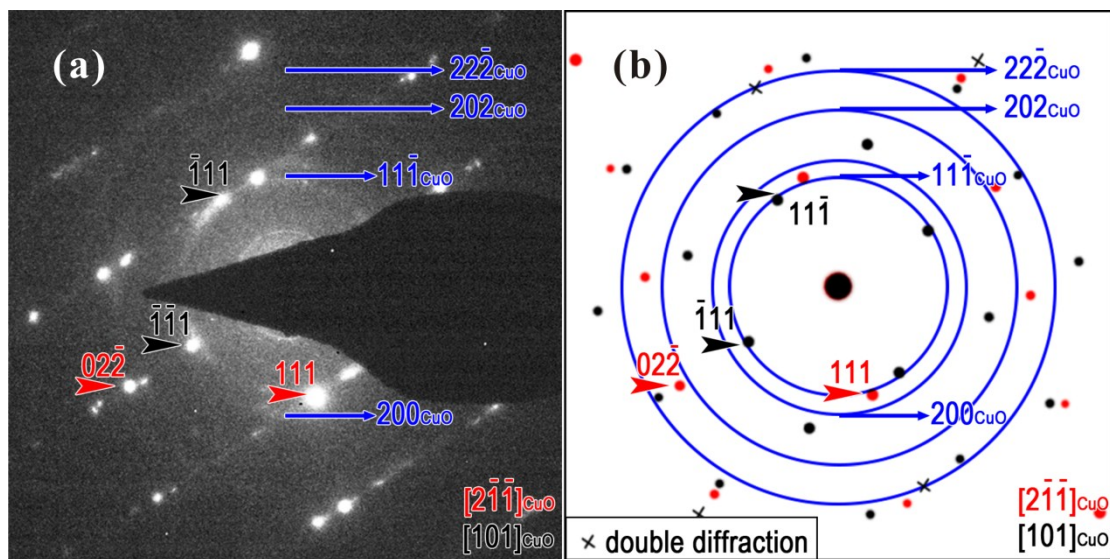


Fig. S6 (a) SAED pattern and (b) simulation results of type III sample.

S7. Further experimental evidence. It is known that thermal annealing under appropriate conditions can cause recrystallization and reduce the concentration of defects in bulk materials. We therefore applied this process to the nanowires. We chose laser annealing because it can be aimed at a fixed position on a single nanowire.

The experiment was carried out in the ambient environment on a Raman spectroscope (Renishaw inVia Reflex confocal micro-Raman system) using a 532 nm Ar-ion laser. The exposure time was 5 s, and the diameter of the light spot was approximately 1 μm . The position of the nanowire exposed by the laser is marked by a red circle in Fig. S7 (a).

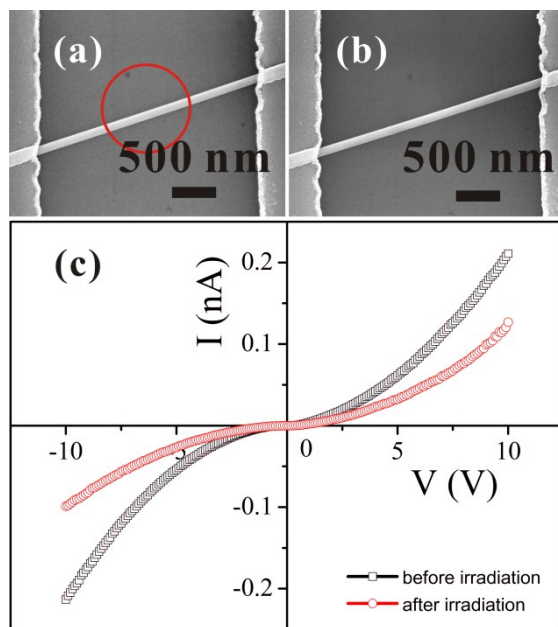


Fig. S7 (a) SEM image of a CuO nanowire before irradiation; the position of the nanowire exposed to the laser is marked by a red circle. (b) SEM image of the CuO nanowire after irradiation. (c) Comparison of the electrical properties of the CuO nanowire before and after irradiation. The curve of black squares is the I - V curve before irradiation, and the curve of red circles is the I - V curve after irradiation.

We characterized the samples by SEM both before and after irradiation, and the results are shown in Fig. S7. The laser power we used was very low, and it is clear from the SEM images that the morphology of the nanowires did not change with irradiation. However, the measured electrical properties of the nanowires showed an obvious decrease in conductance. The value of E_a calculated by thermal activation theory changed from 243.1 meV to 313.9 meV. From a comparison of the I - V curves, and from values of E_a calculated for the CuO nanowire before and after irradiation, we conclude that the sample after laser irradiation has undergone recrystallization.

After being exposed to the laser, water molecules in the ambient environment around the sample may be ionised, and the dissociated hydrogen atoms can react with redundant oxygen atoms in the CuO nanowire, reducing the number of defects in the nanowire and thus decreasing the defect concentration. Therefore, the proportion of thermal activation increases after irradiation, and the transport mechanism for this sample tends to change from type III to type II, depending on the variation in the defect concentration. This leads to a change in the conductivity after the laser process. This experiment provides evidence to confirm the mechanism we propose in the main text of this manuscript.

References

1. S. Sinha, S. K. Chatterjee, J. Ghosh and A. K. Meikap, *Journal of Applied Physics*, 2013, **113**, 123704.
2. X. M. Song and J. Chen, *Applied Surface Science*, 2015, **329**, 94-103.